

THE DEVELOPMENT OF A SPATIO-TEMPORAL MODEL FOR WATER HYACINTH BIOLOGICAL CONTROL STRATEGIES

HELÉNE VAN SCHALKWYK¹, LINKE POTGIETER¹, CANG HUI^{2,3}

¹Department of Logistics, Stellenbosch University, South Africa

²Department of Mathematical Sciences, Stellenbosch University, South Africa

³African Institute for Mathematical Sciences, South Africa

ABSTRACT. A reaction-diffusion model for a temporally variable and spatially heterogeneous environment is developed to mathematically describe the spatial dynamics of water hyacinth and the interacting populations of the various life stages of the *Neochetina eichhorniae* weevil as a biological control agent on a bounded two-dimensional spatial domain. Difficulties encountered during the implementation of the model in MATLAB are discussed, including the implementation of time delays and spatial averaging. Conceptual validation tests indicate that the model may succeed in describing the spatio-temporal dynamics of the water hyacinth and weevil interaction. A modelling framework is thereby provided to evaluate the effectiveness of different biological control release strategies, providing guidance towards the optimal magnitude, timing, frequency and distribution of agent releases. Numerical results confirm the hypothesis that the seasonal timing of releases have a significant influence on the success of the control achieved. However, in order to ascertain the degree to which the model output realistically represent the real life water hyacinth and weevil interaction, predictive validation tests are proposed for further research.

Keywords: Biological control, water hyacinth, reaction-diffusion model, optimal release strategy

1 INTRODUCTION

Water hyacinth, *Eichhornia crassipes* (Martius) Solms-Laubach (Pontederiaceae), has since the 1880s been distributed from its Amazonian origin to all parts of the world. Today it is regarded as one of the world's, as well as South Africa's, worst aquatic weeds. With its exponentially high growth rate, water hyacinth rules still or slow-moving water bodies by forming dense impenetrable mats across the surfaces, having serious consequences for man and animal. Given enough space and favourable growing conditions (tropical weather, warm temperatures and water with high nutrient levels), the number of plants may double in a matter of a week, giving water hyacinth the ability to outgrow any native species occurring in the system. Seeds can remain viable after 15 – 20 years of remaining in water sediments [12, 15]. These characteristics make water hyacinth an extremely difficult weed to control.

Over the past century, mechanical, chemical and manual control methods proved to be both very expensive and ineffective, especially for large infested water bodies. These concerns motivated a more serious consideration of the use of biological control methods [13].

Biological control entails the sourcing of natural enemies from the weed's native land and putting them through quarantine where their host specificity is assessed. If proven to be host specific, they are certified for release as biological control agents (BCAs) for the specific weed. Candidate species are then released in the new habitat where they feed on the weed, thereby contributing to the suppression of the alien plant population. After extensive research began in Argentina in 1961, the first water hyacinth host-specific natural enemies were released as BCAs in the USA in the early 1970s. Since then several BCAs have been released in 33 countries [13]. Biological control trumps other methods by offering a more sustainable, long-termed, environment-friendly and more affordable solution to the water hyacinth problem, even for large or inaccessible areas [10].

Apart from the classical biological control approach, where BCAs are released in the field directly out of quarantine, the use of mass rearing technology in biological control has become more common. BCAs that have been cleared from quarantine are taken to a mass rearing facility where aquatic weed BCAs are reared in large numbers on their host plants in portable pools, mak-

ing more frequent releases possible in order to speed up biological control [3]. Inadequate release methods may cause non-establishment of BCAs or unsuccessful control [10]. Therefore, implementing the best timing, frequency, magnitude and distribution for releases are vital to a successful biological control programme.

The biological control of water hyacinth in South Africa currently relies on six agents of which the popular *Neochetina eichhorniae* Warner (Coleoptera: Curculionidae) weevil species is considered in this paper. The sound and effective management of the water hyacinth weed remains a challenge in South Africa [3]. A local mass rearing facility from the Cape Town *Invasive Species Unit* in Westlake commenced with weekly releases of BCAs at the nearby Kuilsriver site in March 2015 [14]. After one and a half years of BCA releases, consisting of mostly *Megamelus scutellaris* Berg (Hemiptera: Delphacidae) (more than 380 000) and a few *Neochetina bruchi* Hustache (Coleoptera: Curculionidae) weevils (about 2 600), the site was still completely covered with water hyacinth, with little evidence of the impact of BCAs. Suggestions towards more effective release strategies for different temperature conditions may aid in improving the control of the weed. Byrne et al. [2] agrees that flawed or inappropriate release procedures contribute to the variable success of biological control programmes for water hyacinth. It is hypothesized that the timing of releases, both in terms of seasonality and frequency of releases, have a significant influence on the success of the control achieved.

In this paper, a mathematical model, describing the water hyacinth and *N. eichhorniae* weevil population growth, dispersal and interaction in a temporally variable and spatially heterogeneous environment, is proposed to provide guidance towards how the weevils can be optimally utilised as BCA in South Africa. Model simulations may be used to investigate the efficiency of different BCA release strategies for different temperature conditions, and given the environmental conditions, to provide guidance towards the optimal magnitude, frequency, seasonal timing and spatial distribution of BCAs

releases. In addition, model simulations may be used to predict whether or not a specific agent will be able to establish in the area of interest. The model presented in this paper builds on previous work by Wilson [21], who presented a stage-structured plant-herbivore model, investigating the population dynamics of water hyacinth and the interaction with the *N. eichhorniae* weevil as BCA in one dimension. The temporal mean-field model developed by Wilson [21] is not realistic in assuming that weevils are uniformly distributed throughout an area, while in reality BCAs are released along the edges of an infested water body. A spatially explicit model is therefore required to model the distribution of water hyacinth and the weevils in a heterogeneous environment.

2 MODELLING APPROACH

The following assumptions concerning the modelling of the water hyacinth and weevil species are made in this paper.

1. *Stage-structure.* The *N. eichhorniae* weevil population is represented by five development stages (Fig. 1), while the water hyacinth population is considered at its mature stage to examine the influence of the weevils on an established water hyacinth population. Individuals in the weevil population enter a stage by developing from the previous stage or by reproduction from the mature stage and leave a stage through death or maturation. By adding stage-structure, the model accounts for more biological detail of the weevils and allows for the explicit modelling of processes pertaining only to specific development stages, making it a more realistic representation. The number of equations necessary to represent the weevil population is limited to the number of development stages that have density-dependent processes. In this paper, similar to the temporal model developed by Wilson [21], the two larval stages and the adult stage are considered sufficient to represent the weevil population.
2. *Plant growth.* Several factors affecting the growth of the water hyacinth are not included in the model as

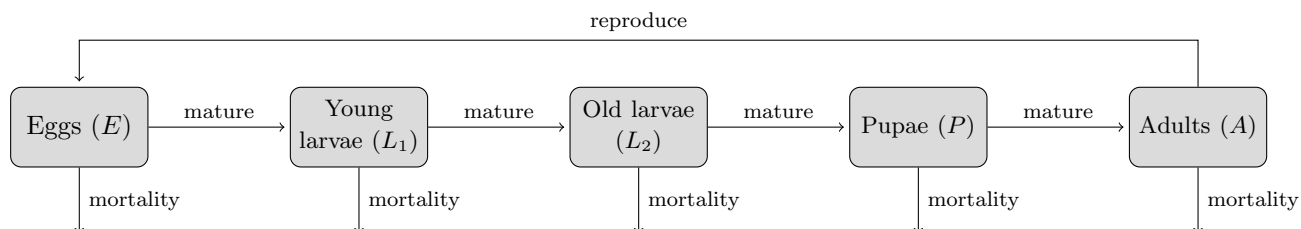


Figure 1: Diagram of the *N. eichhorniae* weevil’s development stages as used in model development.

it is difficult to quantify. These factors include frost, diseases, saltiness of water, wind, humidity, water currents, floods, light and carbon dioxide concentration [12, 21]. Constant nitrogen and phosphorus levels are assumed throughout the study.

3. *Damage factor.* While both the *N. eichhorniae* larvae and adults feed on water hyacinth, it is assumed that only the old larvae cause actual damage to the plant. In addition to the removal of biomass, tunnelling of larvae into the petioles and the crown of the plant can cause nutrient deficiency as well as provide a route of entry for disease-causing microorganisms. The movement of larvae between leaves and the crown of the plant may also lead to flooding of larval tunnels and a reduction in plant buoyancy [21]. Feeding by adults on the outside of the leaves does not directly affect the rhizome or the meristem of the plant, both of which may be damaged by larval feeding. In most cases, adult feeding appears to be much less destructive to water hyacinth and is thought to be negligible compared to damage caused by old larvae [4, 21].
4. *Ovipositing.* Adult weevils are assumed to start laying eggs immediately after they enter the system and continue to oviposit at a constant rate throughout their lifetime. The oviposition rate is adjusted accordingly to allow females to lay the approximated maximum amount of eggs during their lifetime.
5. *Reproduction.* When adult density within a considered area decreases below a minimum threshold, it is assumed that they will not be able to reproduce any longer. There has to be a sufficient number of adults within a reachable range of each other for reproduction to occur.
6. *Density dependence.* From experiments and personal observations, Wilson [21] found it reasonable to assume that due to adult weevil mobility, the female weevils will oviposit regardless of density, resulting in density-independent oviposition and egg survival rates for any realistic density of adults per plant. Due to the relative mobility of old larvae, the through-stage survival rates of the old larval and pupal stages of the weevil's life cycle are also assumed unaffected by density. Density-dependent mortality is only added to the young larval population as Wilson [21] found that most density dependence occurs before damage is caused to the plant. At high larval densities, young larvae may have a higher probability of being stranded in decaying leaves. It is assumed that adults have abundant supplies of any limiting nutrient.
7. *Dispersal.* The presented spatio-temporal model assumes that individuals in the mobile development stages of the weevil population perform an unbiased random walk. This assumption concurs with previous studies which found that weevils randomly disperse throughout a water hyacinth mat without any apparent preference for particular areas of the plants [9]. During each time unit, a proportion of old larvae and adult weevils are assumed to leave their current location to inhabit neighbouring sites within their reach. This motion can be modelled in terms of *Fickian diffusion* and is approximated by using the Laplacian operator. The water hyacinth dispersal is also described by Fickian diffusion as weed mats randomly expand to neighbouring sites.
8. *Domain.* For the demonstrative purpose of this study, the spatial domain is assumed to be an isolated rectangular water body infested with water hyacinth to its carrying capacity, surrounded by land use categories considered unsuitable habitat for water hyacinth or *N. eichhorniae* weevils. It is thus assumed that neither plant nor weevil enters or exits the domain. The spatial domain is considered heterogeneous as the plant or weevil densities may vary for different locations due to the fact that weevils are not uniformly spread across an area.
9. *Releases.* Adult weevils are released by hand from small plastic containers at the accessible edges of an infested water body and take time to disperse to neighbouring sites. In some cases, boats may be used for releases on larger water bodies. Releases are assumed to occur once off or at a constant rate over the period of release. The distribution of the releases may be influenced by the accessibility to the infested area and the number of available BCAs.

2.1 Model formulation and notation Let $W(\underline{\xi}, t)$ denote the biomass density of water hyacinth material (in kg/unit²) at location $\underline{\xi} = [\xi_1, \xi_2]^T \in \mathcal{D}$ at time t , where \mathcal{D} is a closed, two-dimensional spatial domain, and $E(\underline{\xi}, t)$, $L_1(\underline{\xi}, t)$, $L_2(\underline{\xi}, t)$, $P(\underline{\xi}, t)$ and $A(\underline{\xi}, t)$ denote the densities of eggs, young larvae, old larvae, pupae and adult weevils at location $\underline{\xi}$ at time t , respectively. Similar to the modelling approach for a variable survival rate used in previous studies [8, 21], let $S_{L_1}(\underline{\xi}, t)$ denote the density-dependent through stage survival rate for young larvae at location $\underline{\xi}$ at time t . All other development stages are assumed to have density-independent per capita death rates, yielding constant survival rates. Time delays are modelled as differences from the current time t and subscripts indicate the stage involved, *e.g.* the development duration of the egg stage is denoted

by t_E . The time spent in each stage of the weevil’s life cycle is temperature-dependent.

In order to model the spatial dynamics of the water hyacinth and weevil system in a bounded two-dimensional spatial domain, diffusion terms are added to the applicable ordinary delay differential equations in the temporal model presented by Wilson [21]. Let the diffusion coefficients d_W , $d_{L_2}(\theta)$ and d_A be a measure of how effectively water hyacinth, old larvae and adult weevils disperse between neighbouring locations, respectively, invariant in time and space. In addition, an Allee-effect and a term allowing for frequent releases of adult weevils are included, a more detailed temperature dependence is incorporated, as well as slight changes to the modelling of the through stage survival probabilities. Furthermore, a different approach towards the modelling of the recruitment and maturation terms for the weevil population is followed and a sufficient expression for the old larval maturation term with dispersal is derived.

Let $R_i(\xi, t)$ denote the rate of recruitment into stage i of the weevil’s life cycle at location ξ at time t . The rate of recruitment into the young larval stage at location ξ at time t is equal to the number of eggs maturing at the corresponding location and time. The number of eggs maturing is the number of eggs laid at location ξ and $t_E(\theta)$ days ago – the number of adults present at that location $t_E(\theta)$ days ago multiplied by the oviposition rate – multiplied by the probability of surviving through the egg stage. The young larval recruitment rate is limited by an Allee-effect, resulting in a decrease of the young larval population growth rate at low adult weevil densities. Once the adult population within a considered area of 1 m^2 falls below the minimum threshold for reproduction, a , the negative instantaneous growth rate of the young larvae leads to the extinction of the population. The Allee-effect may cause slower spread and decreased establishment likelihood of BCAs, influencing the efficacy and cost of biological control. Expected spatial ranges, distributions and patterns of species may be altered when an Allee-effect is present [19], making this an important effect to consider. The rate of maturation out of the young larval stage at location ξ at time t , which is equal to the recruitment rate into the old larval stage at location ξ at time t , is simply the recruitment rate into the young larval stage at time $t - t_{L_1}(\theta)$ multiplied by the probability of surviving through the young larval stage. The same logic is followed for the recruitment and maturation rates of the other weevil development stages, except for the maturation rate out of the old larval stage where diffusion is involved. The time-delay term for this rate of maturation must be derived in a different way because an old larva can move during the period between entering the system and maturing

to the next stage and is therefore expected to enter the pupal stage at a point in space different from where it originally emerged. The recruitment rates used in the model are given by

$$R_{L_1}(\xi, t) = q(\theta)A(\xi, t - t_E(\theta))\sigma_E(\theta) \left(\frac{A(\xi, t - t_E(\theta)) - a}{A(\xi, t - t_E(\theta))} \right), \quad (1)$$

$$R_{L_2}(\xi, t) = \begin{cases} R_{L_1}(\xi, t - t_{L_1}(\theta)) S_{L_1}(\xi, t) & \text{if } R_{L_1}(\xi, t - t_{L_1}(\theta)) > 0, \\ 0 & \text{otherwise,} \end{cases} \quad (2)$$

$$R_P(\xi, t) = \bar{R}_{L_2}(\xi, t) \sigma_{L_2}(\theta), \quad (3)$$

$$R_A(\xi, t) = R_P(\xi, t - t_P(\theta)) \sigma_P(\theta), \quad (4)$$

where θ denotes the temperature (in $^{\circ}\text{C}$), $q(\theta)$ the rate of oviposition of viable eggs at temperature θ , $t_i(\theta)$ the development duration in days of stage i of the weevil’s life cycle at temperature θ and $\sigma_i(\theta)$ the density-independent through stage survival probability for stage i at temperature θ . The calculated development durations of immature stages at different temperatures are given in Table 1.

Table 1: Development duration of weevil life stages, measured at different temperatures.

Temp ($^{\circ}\text{C}$)	Development duration (in days)			
	Eggs (t_E)	Young larvae (t_{L_1})	Old larvae (t_{L_2})	Pupae (t_P)
16.00	44.00	47.00	35.00	33.00
20.00	24.00	47.00	25.87	29.85
25.00	12.00	28.85	14.42	19.90
30.00	8.00	20.00	10.00	14.93
35.00	16.00	40.00	20.00	29.85
39.00	44.00	47.00	35.00	33.00

Provided the maximum probability of surviving through stage i , attained from Wilson [21], the change in the survival probabilities $\sigma_i(\theta)$ as a result of changes in temperature was determined and is shown in Figure 2.

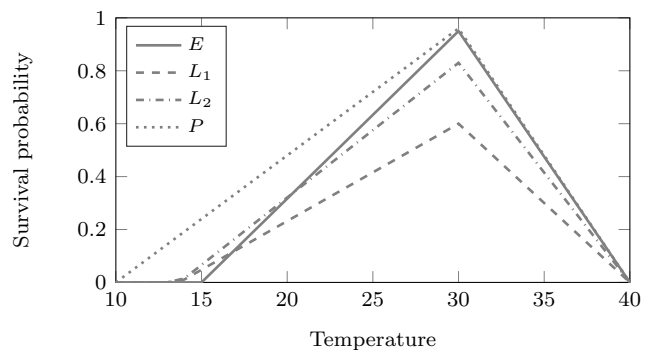


Figure 2: Through stage survival probabilities, measured at different temperatures.

The reaction-diffusion model for the interacting species, formulated as a system of coupled delay partial differential equations (PDEs), linked to the set of algebraic equations (1) – (4), is given by

$$\frac{\partial W(\underline{\xi}, t)}{\partial t} = d_W \nabla^2 W(\underline{\xi}, t) + r(\theta)W(\underline{\xi}, t) \left(1 - \frac{W(\underline{\xi}, t)}{K}\right) - c_{L_2}(\theta)L_2(\underline{\xi}, t) \left(\frac{W(\underline{\xi}, t)}{W(\underline{\xi}, t) + H}\right), \quad (5)$$

$$\frac{\partial L_1(\underline{\xi}, t)}{\partial t} = R_{L_1}(\underline{\xi}, t) - \left(\mu_{L_1}(\theta) + \frac{J_{L_1}}{W(\underline{\xi}, t)}L_1(\underline{\xi}, t)\right)L_1(\underline{\xi}, t) - R_{L_2}(\underline{\xi}, t), \quad (6)$$

$$\frac{\partial L_2(\underline{\xi}, t)}{\partial t} = d_{L_2}(\theta)\nabla^2 L_2(\underline{\xi}, t) + R_{L_2}(\underline{\xi}, t) - \mu_{L_2}(\theta)L_2(\underline{\xi}, t) - R_P(\underline{\xi}, t), \quad (7)$$

$$\frac{\partial A(\underline{\xi}, t)}{\partial t} = d_A \nabla^2 A(\underline{\xi}, t) + R_A(\underline{\xi}, t) - \mu_A(\theta)A(\underline{\xi}, t) + IX(\underline{\xi}, t), \quad (8)$$

$$\frac{\partial S_{L_1}(\underline{\xi}, t)}{\partial t} = S_{L_1}(\underline{\xi}, t) J_{L_1} \left(\frac{L_1(\underline{\xi}, t - t_{L_1}(\theta))}{W(\underline{\xi}, t - t_{L_1}(\theta))} - \frac{L_1(\underline{\xi}, t)}{W(\underline{\xi}, t)} \right), \quad (9)$$

where $\nabla^2 \equiv \frac{\partial^2}{\partial \xi_1^2} + \frac{\partial^2}{\partial \xi_2^2}$ denotes the Laplacian operator for diffusion, $r(\theta)$ the daily intrinsic growth rate of the plant at temperature θ and K the carrying capacity (kg/unit²) of the water resource. Furthermore, $c_{L_2}(\theta)$ denotes the rate of damage caused by the older larvae at temperature θ and H the plant density at which herbivore feeding is reduced by half. Parameters $q(\theta), r(\theta), K, c_{L_2}(\theta), H$ and J_{L_1} were obtained from Wilson [21].

Assuming a given young larva competes equally with all other young larvae for limited resources, Gurney et al. [8] suggested to reflect this limitation by choosing a per capita young larval death rate which varies linearly with young larval population. In line with Wilson’s application of this modelling approach [21], the young larval density-dependent mortality rate is given by $\frac{J_{L_1}}{W(\underline{\xi}, t)}L_1(\underline{\xi}, t)$, where J_{L_1} denotes the density-dependent scaling parameter for young larvae which is equal to the number of kilograms of plant material per young larva at which the young larval population growth rate is zero. In equations (6) – (8), $\mu_i(\theta)$ denotes the daily density-independent mortality rate for stage i ($i = L_1, L_2$ or A) of the weevil’s life cycle at temperature θ and is given by

$$\mu_i(\theta) = \begin{cases} -\frac{\ln(\sigma_i(\theta))}{t_i(\theta)} & \text{if } \sigma_i(\theta) > 0 \\ 1 & \text{otherwise.} \end{cases}$$

Finally, I denotes the number of new adult weevils released per location at any time and

$$X(\underline{\xi}, t) = \begin{cases} 1 & \text{if BCAs are released at location } \underline{\xi} \\ & \text{at time } t \\ 0 & \text{otherwise.} \end{cases} \quad (10)$$

Since the state variables $W(\underline{\xi}, t), L_1(\underline{\xi}, t), L_2(\underline{\xi}, t)$ and $A(\underline{\xi}, t)$ represent population densities, they are set to be non-negative real numbers for obvious reasons. The density-dependent survival rate, $S_{L_1}(\underline{\xi}, t)$, is assumed to have a lower bound of zero and an upper bound equal to the density-independent through stage survival rate for young larvae, $\sigma_{L_1}(\theta)$.

Based on Gourley & Kuang’s [5] formulation of a bounded one-dimensional single-species diffusive-delay population model, the time-delayed maturation term for the old larval stage where there is diffusion is derived for the model in a closed, two-dimensional spatial domain \mathcal{D} with homogeneous Neumann boundary conditions. For simplicity’s sake, studies in literature only demonstrate the derivation of the delay term for a one-dimensional domain [5, 7], only mentioning that it should be possible to carry out numerical simulations in higher space dimensions.

In algebraic equation (3), the weighted average of R_{L_2} at an earlier time is given by

$$\bar{R}_{L_2}(\underline{\xi}, t) = \int_{\mathcal{D}} G(\underline{\xi}, \underline{x}, t_{L_2}(\theta)) R_{L_2}(\underline{x}, t - t_{L_2}(\theta)) d\underline{x}, \quad (11)$$

where \underline{x} is another point in space. Old larvae will have emerged at various locations (\underline{x}) in domain \mathcal{D} and may have moved around, being at point $\underline{\xi}$ on maturing to the pupal stage. The quantity $\bar{R}_{L_2}(\underline{\xi}, t)\sigma_{L_2}(\theta)$ gives the rate at which old larvae mature into the pupal stage at location $\underline{\xi}$ and time t , having taken $t_{L_2}(\theta)$ days to mature. The spatial averaging function $G(\underline{\xi}, \underline{x}, t)$ is the solution of

$$\frac{\partial G}{\partial t} = d_{L_2}(\theta)\nabla^2 G, \quad (12)$$

subject to homogeneous Neumann boundary conditions and initial conditions given by

$$G(\underline{\xi}, \underline{x}, 0) = \delta(\underline{\xi} - \underline{x}), \quad (13)$$

where δ is the Dirac delta function and ∇^2 the Laplacian computed with respect to the first argument of $G(\underline{\xi}, \underline{x}, t)$. The Dirac delta function, $\delta(\underline{\xi} - \underline{x})$, has the value 0 for all $\underline{\xi} \neq \underline{x}$ and 1 for $\underline{\xi} = \underline{x}$. Furthermore, function $G(\underline{\xi}, \underline{x}, t) > 0$ for all $t > 0$. If $R_{L_2}(\underline{\xi}, s) \geq 0$ for all $\underline{\xi} \in \mathcal{D}$ and $s \leq t$, then $\bar{R}_{L_2}(\underline{\xi}, t) \geq 0$. This follows from the positivity of G . Although the explicit expression of the spatial averaging kernel $G(\underline{\xi}, \underline{x}, t)$ is difficult to compute (or unknown) for the bounded two-dimensional case, literature indicates that it is only necessary to know that the function G is the solution of equation (12) subject to (13) [1, 7].

According to Gourley & Kuang [6], the existence of solutions to one-dimensional delay reaction-diffusion systems, similar to the one described in equations (5) – (9), which is already more complex due to being in two dimensions, have yet to be established. It is therefore assumed that a solution to the presented model exists and the focus in the rest of the thesis is turned towards how the model may be applied to optimise water hyacinth biological control release strategies.

A limitation of the time-delayed modelling approach is that time lags allow weevil populations to still exist for a period of time at a specific location after the plant has been driven to extinction at that point in space, as density dependence in terms of limiting resources is only added to the young larval stage. There is a delayed density dependence effect on the other weevil development stages. In the long term, these delayed effects become negligible and the model still succeeds in providing good estimates of the overall population dynamics.

2.1.1 Boundary conditions Since water hyacinth cannot exist on land and *N. eichhorniae* weevils are host-specific BCAs, only able to survive on water hyacinth, it is assumed that neither plant nor weevil enters or exits the domain. System (5) – (9) is therefore subject to homogeneous Neumann boundary conditions given by

$$\underline{n} \cdot (\mathbf{D} \otimes \nabla \underline{u}) = \underline{0}, \quad \forall \underline{\xi} \in \partial \mathcal{D}, \quad (14)$$

where \underline{n} is the outward normal vector on the boundary, \mathbf{D} the diffusion coefficient matrix, \underline{u} the solution of the system and $\partial \mathcal{D}$ the boundary of \mathcal{D} .

2.1.2 Initial conditions Initially the water hyacinth density is assumed to be at carrying capacity ($K = 70 \text{ kg/m}^2$) throughout the whole domain under consideration (\mathcal{D}) and all weevil stages are assumed absent prior to BCA releases. A certain amount of adult weevils will be released at specific locations at the edges of the domain at time $t = 0$. The initial conditions for system (5) – (9) are thus given by

$$\begin{aligned} W(\underline{\xi}, t) &= K, & \text{for } t \leq 0, & \quad \forall \underline{\xi} \in \mathcal{D} \\ L_1(\underline{\xi}, t) &= 0, & \text{for } t \leq 0, & \quad \forall \underline{\xi} \in \mathcal{D} \\ L_2(\underline{\xi}, t) &= 0, & \text{for } t \leq 0, & \quad \forall \underline{\xi} \in \mathcal{D} \\ A(\underline{\xi}, t) &= 0, & \text{for } t < 0, & \quad \forall \underline{\xi} \in \mathcal{D} \\ A(\underline{\xi}, 0) &= \begin{cases} I & \text{if } X(\underline{\xi}, 0) = 1 \\ 0 & \text{otherwise} \end{cases} \\ \sigma_{L_1}(\underline{\xi}, t) &= \sigma_{L_1}(\theta), & \text{for } t \leq 0, & \quad \forall \underline{\xi} \in \mathcal{D}, \end{aligned} \quad (15)$$

where K, I and $\sigma_{L_1}(\theta)$ are assumed to be positive real numbers.

3 SOFTWARE IMPLEMENTATION

The model was implemented in MATLAB 9.0 (R2016a) where the system of coupled delay PDEs in a bounded

two-dimensional spatial domain is solved using tools from the PDE toolbox and its built-in functions [20]. Various difficulties encountered during the implementation process are discussed below.

1. *System formulation.* Firstly, the equations had to be put in the correct form in order to be able to use tools from MATLAB’s PDE toolbox to solve the system of PDEs, since the toolbox does not have the option for solving nonlinear parabolic PDEs. For each equation, the linear part is put on the left-hand side and the nonlinear part on the right-hand side of the equation. Similar to an approach used by Howard [11], the nonlinearity is taken as a driving term from the previous time step and the remaining linear equations are decoupled so that 5 single equations are solved rather than a system. Provided the initial conditions, solution times, boundary conditions, mesh parameters and various PDE coefficients, the built-in `parabolic` function produces the solution to the *finite element method*¹ formulation of the PDE problem. The `parabolic` function creates finite element matrices corresponding to the problem internally and calls `ode15s` to solve the resulting system of ordinary differential equations.
2. *Time lags.* Since the built-in functions do not allow for time lags, history matrices containing the solutions to the system at all previous time increments are constructed to determine the partial derivative of a function where the solution at a certain time depends on the values of the function at previous times.
3. *Spatial averaging.* Spatial averaging for the old larvae stage, involving both time delay and diffusion, had to be implemented. An explicit expression for the spatial averaging kernel $G(\underline{\xi}, \underline{x}, t_{L_2}(\theta))$ in equation (11) in the bounded two-dimensional case does not exist. Therefore, the expression for the spatial averaging kernel for the *unbounded* case is used in the implementation and the effect of each reflecting boundary (homogeneous Neumann boundary conditions) is accounted for manually. Following an approach used by Powell [16], the effect of reflecting boundaries are simulated by creating artificial populations of dispersers on the outsides of the boundaries, which, when they disperse back toward the original grid, will add to the original population the individuals that “reflected” from the boundaries. This is accomplished by first reflecting the

¹The finite element method (FEM) is a numerical technique for finding approximate solutions to PDEs when finding their solutions by analytical means is impossible. FEM subdivides a large problem into smaller, simpler parts and approximates a solution to the problem by minimising an associated error function [18].

data of the original grid over each boundary, storing the reflections together with the original grid (nine grids in total) in an artificial grid and considering the new grid as an infinite domain. Spatial averaging is then performed over the entire new grid. Finally, the original grid is extracted to obtain the population of interest. The effect of what happens at each boundary of the original grid is illustrated in Figure 3, with a reflecting boundary at 0. The red line resembles the initial population at time 0, blue the dispersal of the original population after a certain time period, green the dispersal of the reflected population and magenta the final population of interest, which is the population after dispersal, taking the reflecting boundaries into account. The final population distribution (magenta) is the sum of the original (blue) and reflected (green) population densities for each location within the original grid.

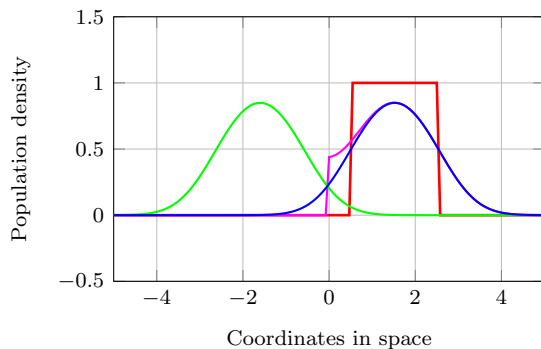


Figure 3: Illustration of how the effect of a reflecting boundary is accounted for in the model.

The recruitment rate $R_{L_2}(\underline{x}, t - t_{L_2}(\theta))$ is considered as the initial population for the old larval stage. The individuals disperse randomly according to the distribution g . Derived from the one-dimensional unbounded expression provided in [5, 6] and similar to an expression used by [16], the spatial averaging Gaussian kernel g for the two-dimensional unbounded case is given by

$$g(\underline{\xi}, t_{L_2}(\theta)) = \frac{1}{4\pi d_{L_2} t_{L_2}(\theta)} e^{-(\xi_1^2 + \xi_2^2)/4d_{L_2} t_{L_2}(\theta)}, \quad (16)$$

with parameters as defined in §2.1. The final population distribution after $t_{L_2}(\theta)$ days is given by

$$\int_{-\infty}^{\infty} \int_{-\infty}^{\infty} g(\underline{\xi}, \underline{x}, t_{L_2}(\theta)) R_{L_2}(\underline{x}, t - t_{L_2}(\theta)) d\underline{x} \quad (17)$$

$$= R_{L_2}(\underline{\xi}, t - t_{L_2}(\theta)) * g(\underline{\xi}, t_{L_2}(\theta)),$$

where the latter operation is called the convolution. Algorithm 1 describes the spatial averaging process.

4. *Frequent releases.* Implementing frequent releases for the spatially explicit domain proved to be more

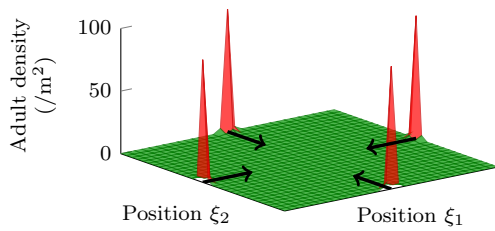
Algorithm 1: Spatial averaging for old larval stage

Input : Distribution of L_2 as they enter the stage at an earlier time, mesh coefficients, development duration of L_2 stage, L_2 diffusion rate.

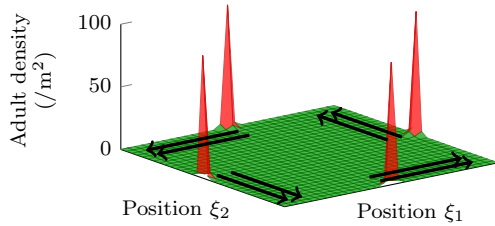
Output: Distribution of L_2 ready to mature at current time.

- 1 Create two-dimensional $a \times b$ grid of geometry;
 - 2 Create triangular mesh of grid;
 - 3 Set $R_{L_2}(i, t - t_{L_2}(\theta))$ as initial population for each node i of the grid;
 - 4 Define expression \mathbf{g} given in Eq. (16) for spatial averaging kernel over entire mesh;
 - 5 Normalise kernel using the built-in `trapz` function;
 // `g/trapz(trapz(g))`
 - 6 Perform Fast Fourier Transform of \mathbf{g} in two dimensions for convolution in Eq. (17); // `fft2(g)`
 - 7 Create reflections of the original grid data over each boundary;
 - 8 Store the reflected grids together with the original grid in a new $3a \times 3b$ grid in their corresponding positions;
 - 9 Perform dispersal on the entire $3a \times 3b$ grid;
 - 10 Extract the original grid's data;
-

challenging than for the spatially implicit case, especially concerning the locations of releases. Releases cannot occur at constant points in the spatial domain as after a period of time the plant may not exist at those points anymore, making it senseless to continue releases at the original points. To account for this, the function of the variable $X(\underline{\xi}, t)$ in equation (10), indicating whether or not a release occurs at location $\underline{\xi}$ at time t , is essentially being implemented by executing two separate procedures. The first procedure determines the *time increments* at which releases are permitted (1 if permitted, 0 otherwise) and the second procedure validates the *locations* of releases (1 for a valid location, 0 otherwise). Concerning the latter procedure, an algorithm was constructed to search for the closest points to the original points of release where there exist sufficient plant densities for releases. The search may be conducted either straight in the direction of the centre of the domain (Fig. 4(a)), or first to the right of the original points of release before it proceeds to the next row towards the centre of the domain, where it again will search to the right and so the process will continue until it reaches the centre of the domain (Fig. 4(b)). Figure 4 illustrates an example of adult releases at the midpoints of each of the four edges of a square domain, with arrows indicating the two options for the directions in which the algorithm may proceed when searching for feasible points of release at each edge of the geometry once plant densities become insufficient at the original



(a) To the centre of the domain.



(b) First to the right of every point.

Figure 4: The two options for the direction in which searches for feasible points of release may be conducted when frequent releases are involved.

points of release. Since there was not a significant difference in the outcome between the two search options, the search straight to the centre of the domain was implemented in the interest of multiple releases per edge, where BCAs are already distributed along an edge and releases to the sides of the original positions become redundant. In the main algorithm where the system of PDEs is solved (Algorithm 2), a release is implemented as an addition of I to the right-hand side of the adult weevil population equation if both the required constraints are met at the considered time and location.

In light of these difficulties, let equations (5) – (9), governing the change in $W(\xi, t)$, $L_1(\xi, t)$, $L_2(\xi, t)$, $A(\xi, t)$ and $S_{L_1}(\xi, t)$, respectively, be the five PDEs being solved in the main procedure (Algorithm 2), assuming parameters and variables as defined in §2.1. Let \mathbf{U}_n be the history matrix for the time-dependent results of the n^{th} PDE.

The water hyacinth and weevil system incorporates variable temperature. Algorithm 3 gives more insight into the process being carried out when the TempDep function is called in lines 6 and 13 of the main algorithm. The temperature-dependent parameters used in system (5) – (9) are $r(\theta)$, $c_{L_2}(\theta)$, $q(\theta)$, $d_{L_2}(\theta)$, $t_E(\theta)$, $t_{L_1}(\theta)$, $t_{L_2}(\theta)$, $t_P(\theta)$, $\sigma_E(\theta)$, $\sigma_{L_1}(\theta)$, $\sigma_{L_2}(\theta)$, $\sigma_P(\theta)$, $\mu_{L_1}(\theta)$, $\mu_{L_2}(\theta)$ and $\mu_A(\theta)$. As described in Algorithm 3, the values of these parameters are updated at the beginning of each month when a new average temperature is set.

Algorithm 2: Solving the system of PDEs

Input : Total running time, starting month, magnitude of releases, release frequency, points of release, Allee-effect threshold, initial conditions.
Output: Solutions to the PDEs at every node for every time increment.

```

1 Create two-dimensional grid of geometry;
2 Assign boundary conditions given in Eq. (14) to edges;
3 Create triangular mesh with  $m$  nodes;
4 Create time vector with  $M$  time-stepping increments;
5 Assign constant values to  $K$  and  $J_{L_1}$  used in Eqs. (5)–(9);
6 Call temperature-dependent parameter values for starting month; // TempDep(month,1)
7 for  $i \leftarrow 1$  to  $m$  do
8 | Set initial conditions given in (15) for Eqs. (5)–(9);
9 end
10 Set initial conditions as first column of each  $\mathbf{U}_n$ ;
11 for  $t \leftarrow 1$  to  $M$  do
12 | if time increment a multiple of 30 then
13 | | Update temp. dependent parameter values for new month; // TempDep(month,t)
14 | end
15 | if  $(t-t_E(\theta)-t_{L_1}(\theta)-t_{L_2}(\theta)) > 0$  then
16 | | Perform spatial averaging for  $L_2$ ; // Alg. 1
17 | end
18 | if time increment a multiple of frequency  $f$  then
19 | | Allow additions to adult population  $A$  at time  $t$  (1st procedure for Eq. (10));
20 | end
21 | Determine coordinates for additions to adult population  $A$  (2nd procedure for Eq. (10));
22 | for  $i \leftarrow 1$  to  $m$  do
23 | | Determine nonlinear interactions for  $W$  using Eq. (5);
24 | | if  $(t-t_E(\theta)) > 0$  then calculate  $R_{L_1}(i, t)$  using Eq. (1);
25 | | else  $R_{L_1}(i, t) = 0$ ;
26 | | if  $(t-t_E(\theta)-t_{L_1}(\theta)) > 0$  &  $R_{L_1}(i, t-t_{L_1}(\theta)) > 0$  then calculate  $R_{L_2}(i, t)$  using Eq. (2);
27 | | else  $R_{L_2}(i, t) = 0$ ;
28 | | if  $(t-t_E(\theta)-t_{L_1}(\theta)-t_{L_2}(\theta)) > 0$  then calculate  $R_P(i, t)$  using Eq. (3);
29 | | else  $R_P(i, t) = 0$ ;
30 | | if  $(t-t_E(\theta)) > 0$  then determine nonlinear interactions for  $L_1$  using Eq. (6);
31 | | else nonlinear interactions for  $L_1 = 0$ ;
32 | | if  $(t-t_E(\theta)-t_{L_1}(\theta)) > 0$  then determine nonlinear interactions for  $L_2$  using Eq. (7);
33 | | else nonlinear interactions for  $L_2 = 0$ ;
34 | | if  $(t-t_E(\theta)-t_{L_1}(\theta)-t_{L_2}(\theta)-t_P(\theta)) > 0$  then determine nonlinear interactions for  $A$  using Eq. (8);
35 | | else nonlinear interactions for  $A = 0$ ;
36 | | if  $(t-t_E(\theta)-t_{L_1}(\theta)) > 0$  then determine nonlinear interactions for  $S_{L_1}$  using Eq. (9);
37 | | else nonlinear interactions for  $S_{L_1} = 0$ ;
38 | end
39 | Define nonlinear interaction terms for all  $n$  PDEs at centerpoints of mesh triangles by interpolation using the built-in pdeintrp function;
40 | Solve all  $n$  PDEs with parabolic function;
41 | Set zero as a lower bound for all solutions;
42 | Append new solutions to each  $\mathbf{U}_n$  for all  $n$  PDEs;
43 end

```

Algorithm 3: Temperature-dependent parameters

Input : Starting month, time increments.

Output: Temperature-dependent parameter values, linear interactions and diffusion coefficients.

- 1 Set vector with monthly average temperatures, depending on starting month;
 - 2 **if** *first time increment* **then** // $t=1$
 - 3 Set average temperature θ for first month;
 - 4 Calculate temp. dependent parameter values;
 - 5 Calculate temp. dependent linear interactions for Eqs. (5)–(9);
 - 6 Calculate temp. dependent diffusion coefficients for Eqs. (5)–(9);
 - 7 **else if** *time increment a multiple of 30* **then**
 - // $\text{mod}(t,30)=0$
 - 8 Update average temperature θ for new month;
 - 9 Calculate temp. dependent parameter values;
 - 10 Calculate temp. dependent linear interactions for Eqs. (5)–(9);
 - 11 Calculate temp. dependent diffusion coefficients for Eqs. (5)–(9);
 - 12 **end**
-

4 MODEL CALIBRATION AND TESTING

In §4.1 and §4.2, suitable parameter values for the diffusion coefficients for adult weevils and water hyacinth, respectively, are determined by means of reverse engineering.

4.1 Adult weevil dispersal By means of dispersal experiments, Haag [9] determined that even in the absence of flight muscles, adult weevils are able to move between adjacent plants over a distance of at least 4 m in a course of one month. Information about adult movement over longer distances is still lacking. It is therefore assumed that adult weevils travel a maximum distance of 4 m per month. By means of reverse engineering, a diffusion coefficient of $d_A = 0.09 \text{ m}^2/\text{day}$ was obtained. In Figure 5, the dispersal of adult weevils released within a 1 m^2 area at the edge of an infested water body at time 0, with $d_A = 0.09 \text{ m}^2/\text{day}$, is shown as obtained from the simulation output.

4.2 Water hyacinth population growth Literature indicates that the water hyacinth surface area may increase by an average of 8% per day under good growing conditions [12]. A diffusion coefficient of $d_W = 0.08 \text{ m}^2/\text{day}$ reflects this assumed daily surface expansion. Figure 6 illustrates the population growth of the weed with the obtained diffusion rate without the influence of the BCAs. The red line indicates the carrying capacity of the water body. Once the plant density at a certain location reaches the carrying capacity,

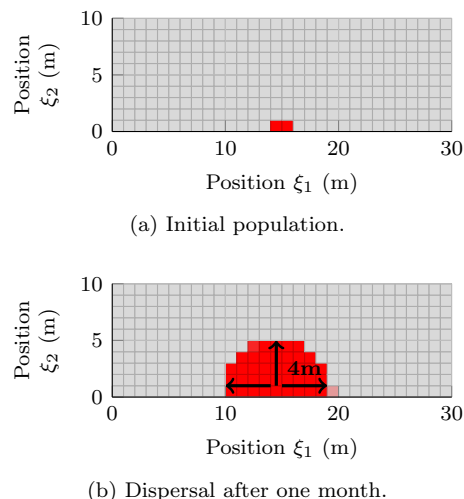


Figure 5: Adult weevil dispersal over one month with the derived diffusion coefficient of $d_A = 0.09 \text{ m}^2/\text{day}$.

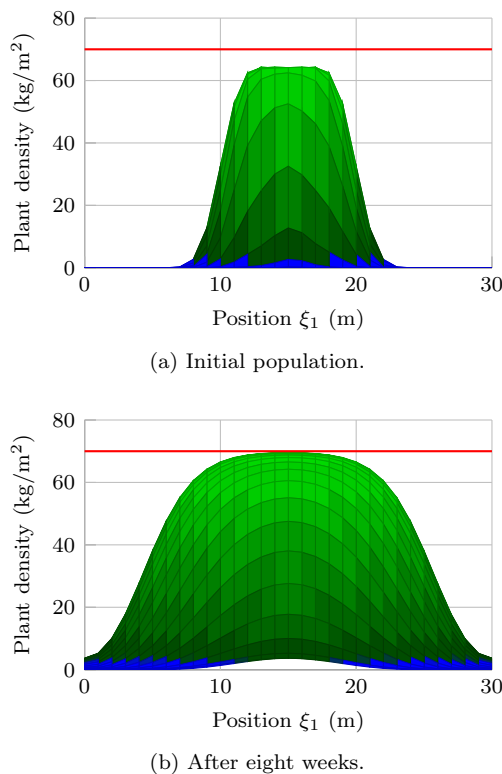


Figure 6: Water hyacinth population growth over eight weeks without BCA releases.

local reactions can no longer contribute to the population growth at that location, but the mat continues to expand sideways through diffusion. The model therefore yields realistic results for water hyacinth growth.

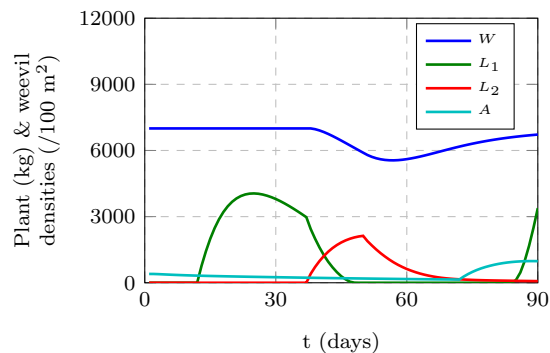
5 MODEL VALIDATION

Conceptual model validation may be described as the process of proving that the theories and assumptions underlying a model yields results within a sufficient range of accuracy, and that the model representation of the real-life problem is sufficient in accordance with the intended purpose of the model. A number of validation techniques exists of which degenerate tests and face validation are used in this paper [17]. A series of degenerate tests were performed to determine whether changes in certain parameter values yield the expected outcome. The effect of different magnitudes of adult releases, temperatures, and release frequencies on controlling water hyacinth are demonstrated in this section. The results from these tests were also compared to experiences in practice, thereby performing face validation. In addition to conceptual validation, these tests demonstrate how the model may be used as a decision-making tool for BCA release strategies.

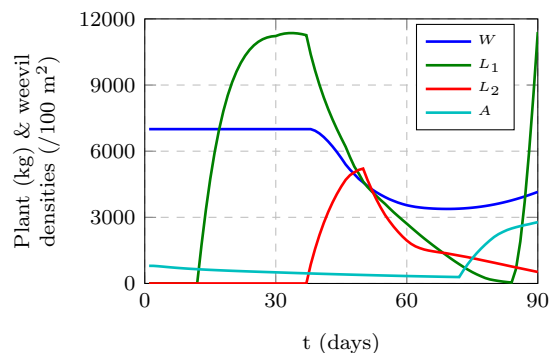
5.1 Effect of different magnitudes of adult releases As a result of more BCAs being present to cause damage, an increase in the magnitude of a release (I) is expected to result in a faster decrease in initial plant density in the short term. For high levels of I , however, density dependence in the young larval stage is expected to result in a faster decrease in weevil population densities compared to lower values of I . In time, decreases in the weevil populations will result in increases in the plant population densities again.

Figure 7 shows the effect of different magnitudes of *N. eichhorniae* adult weevil releases on the total population densities of water hyacinth and the various life stages of the weevil over three months. For both simulations, the applicable number of adults was released in January at the four edges of a 10 m × 10 m area infested with water hyacinth. Young larvae (L_1) appear $t_E(\theta)$ days after adult releases and damage-causing old larvae (L_2) $t_E(\theta) + t_{L_1}(\theta)$ days after initial releases. As the total water hyacinth population decreases due to old larval feeding, density dependence causes a decrease in both larval populations, giving the plant time to increase before the next generation of damaging larvae appear. As expected, model output suggests that releases of 200 weevils at the edges at time 0 will have a greater effect on the total water hyacinth population over a period of three months. Model output also reflects the discernible decreases in water hyacinth populations that were observed after about 70 days in comparable real life release scenarios [3].

The long term plant and weevil densities responses are more variable due to populations being exposed to density-dependent interactions for a longer period of



(a) 100 adults released at each edge.



(b) 200 adults released at each edge.

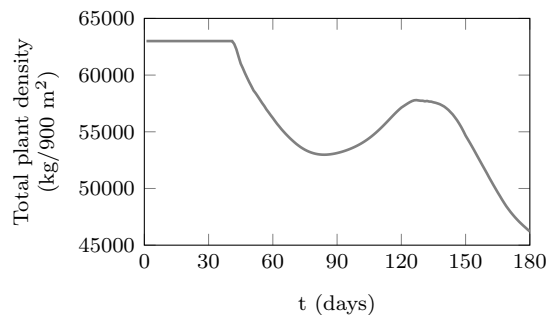
Figure 7: The change in the total plant (W), young larval (L_1), old larval (L_2) and adult (A) population densities over three months for different magnitudes of BCA releases.

time, as expected. The model correctly reflects the hydra effect where an increase in the number of BCAs released does not always result in lower average plant density in the long term due to a greater impact of density dependence on the larval stages when more BCAs are released, yielding less damage-causing old larvae to suppress weed densities.

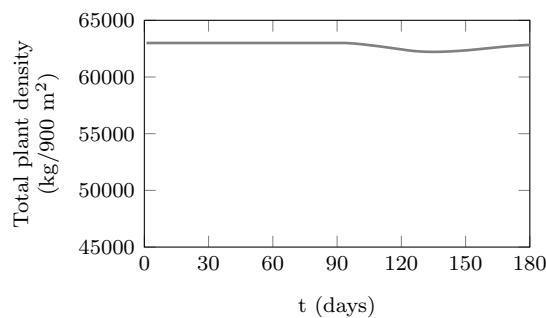
5.2 Effect of temperature on control of water hyacinth Temperature (θ) has an effect on the growth rate of the plant, the weevil oviposition rate, damage rate, survival probabilities, mortality rates and development duration of the weevil stages, as well as the diffusion rate of the old larval stage. For values of θ close to 30°C, the plant will grow at a fast rate, accompanied by a high rate of ovipositing for adult weevils. The development time in each weevil life stage will be shorter than for values of θ deviating from 30°C, with high surviving probabilities and a high old larval daily diffusion rate, resulting in initial weevil infestation levels increasing faster. Since old larvae will cause maximum damage at this level of θ , plant populations are expected to de-

crease fast once old larvae enter the system. Due to density dependence, this should in time result in faster decreases in weevil populations, yielding greater oscillations of population densities.

Simulations were performed to investigate the effect on water hyacinth populations in the Cape Town region when adult weevils are released once-off in summer (December, with an average high temperature of 25°C) or winter (June, with an average high temperature of 18°C), subject to monthly varying temperatures. Once-off releases of 1 000 BCAs at time $t = 0$ at each of the four edges of a 30 m × 30 m infested water body were simulated. Figure 8 illustrate the change in total plant density over six months for summer and winter releases, respectively. It may be seen that the delay between subsequent damage-causing old larval generations gives the weed a chance to grow back. Six months later, the BCAs that were released during summer are exposed to colder winter temperatures, but favourable weather conditions during the first months after releases supported establishment and BCAs could still contribute towards the suppression of weed populations during subsequent colder seasons. Confirming what happens in practice, results (Fig. 8) indicate that BCAs may not be able to establish under certain temperature thresholds due to slower development and higher mortality.



(a) Summer release.



(b) Winter release.

Figure 8: The change in the total plant density over a time period of six months after once-off releases of 1 000 BCAs at four edges in December (a) and June (b).

5.3 Effect of different release frequencies on the control of water hyacinth A direct relationship between the frequency f of BCA releases and the adult weevil population densities is expected. In order to test whether the implementation of the frequent BCA release process responds correctly, simulations were performed with once-off, weekly, two-weekly and four-weekly releases, respectively, with a magnitude of 100 adult weevils per release at each of the four edges of the considered domain and with temperature held constant at 30°C over a period of one year.

As expected, model responses indicate a decrease in the average plant population density over time when BCAs are released more often. In Figure 9, the plant and adult population densities, subject to once-off ($f = 0$), low frequency ($f = 28$) and high frequency ($f = 7$) releases over the period of one year, are shown. Water hyacinth populations are suppressed faster the more often adult weevils are released, as expected. The model succeeds to accurately reflect the regrowth of the weed after a period of time, subsequent to being suppressed to very low densities over the entire domain. Frequent adult weevil releases are ceased once the weed is suppressed below a certain threshold and resumed when the weed grows back to sufficient densities for releases. As expected, higher frequencies of releases result in more effective weed suppressions after regrowth.

6 CONCLUSION

A two-dimensional reaction-diffusion model, formulated as a system of coupled PDEs, was presented in order to describe the population growth and dispersal of water hyacinth and the interacting populations of the development stages of the *N. eichhorniae* weevil as BCA in a temporally and spatially variable environment. Numerical solutions to the system of PDEs in a bounded domain with homogeneous Neumann boundary conditions were obtained by means of simulations of the finite element method implemented in MATLAB. Various challenges in implementing time delays, spatial averaging, frequent releases and fluctuating temperatures were discussed.

Conceptual validation tests indicate that the spatially explicit model may succeed in describing the spatio-temporal dynamics of the water hyacinth and weevil system. Numerical results confirm the hypothesis that the seasonal timing of BCA releases have a significant influence on the success of the control achieved, as well as the magnitude and frequency of the releases. In order to ascertain the robustness of the model output, the next step will be to perform a sensitivity analysis in addition to a predictive validation test of the model output with data from real life release scenarios. Given a realistic repres-

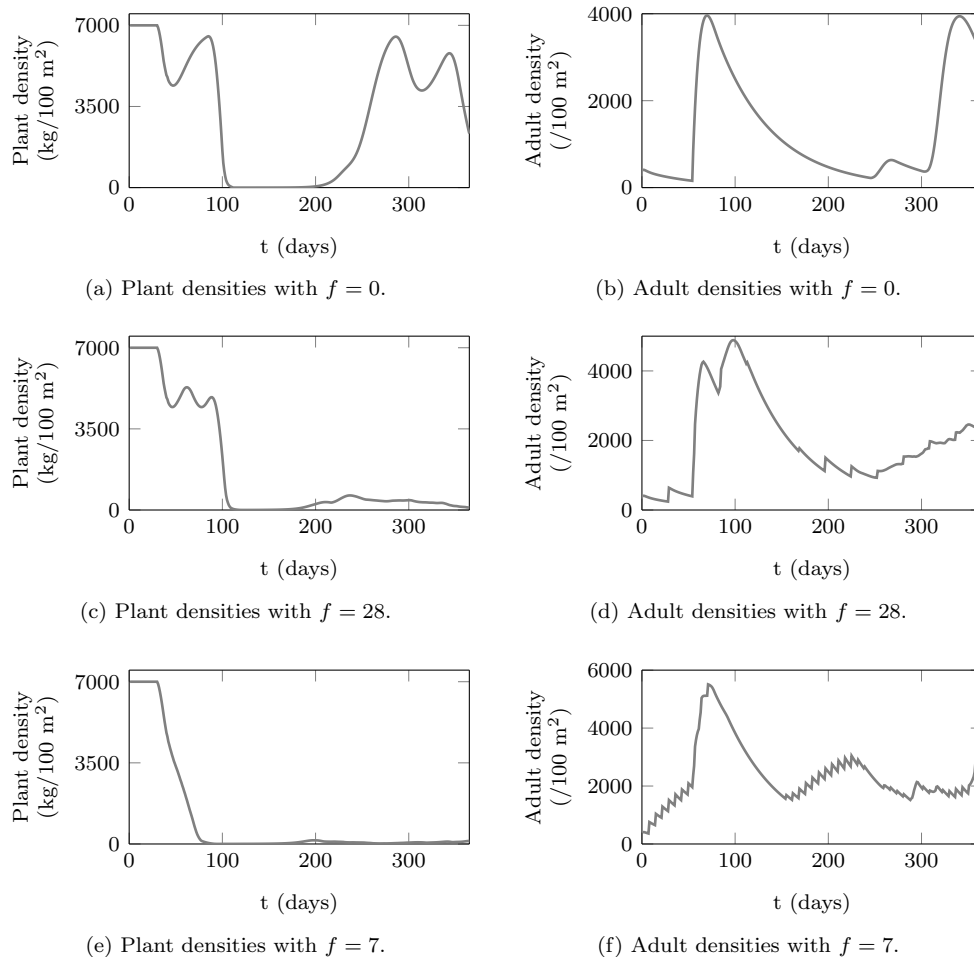


Figure 9: Plant and adult population densities for once-off ($f = 0$), low frequency ($f = 28$) and high frequency ($f = 7$) releases over a time period of one year.

entation of the population growth and dispersal of the interacting species, the model may be used to provide guidance towards the optimal magnitude, frequency, seasonal timing and distribution of BCAs releases.

ACKNOWLEDGEMENTS

We thank Sisanda Nuse from Invasive Species Management who provided insight and information that greatly assisted the research, although she may not necessarily agree with all of the interpretations of this paper. A special thank you to the anonymous reviewers whose insightful feedback notably improved the manuscript.

REFERENCES

[1] Al-Omari, J.F.M. & Gourley, S.A. 2005. A non-local reaction-diffusion model for a single species

with stage structure and distributed maturation delay. *European Journal of Applied Mathematics*. 16(1): 37–51.

[2] Byrne, M., Hill, M., Robertson, M., King, A., Katembo, N., Wilson, J., Brudvig, R., Fisher, J. & Jadhav, A. 2010. Integrated management of water hyacinth in South Africa. WRC Report. (454/10).

[3] Conlong, D.E. 2014. Senior Entomologist at South African Sugarcane Research Institute, Mount Edgecombe, [Personal Communication]. Contactable at des.conlong@sugar.org.za.

[4] DeLoach, C.J. & Cordo, H.A. 1976. Life cycle and biology of *Neochetina bruchi*, a weevil attacking water hyacinth in Argentina, with notes on *N. eichhorniae*. *Annals of the Entomological Society of America*. 69(4): 643–652.

- [5] Gourley, S.A. & Kuang, Y. 2003. Wavefronts and global stability in a time-delayed population model with stage structure. *Proceedings of the Royal Society of London Series A: Mathematical, Physical and Engineering Sciences.* 459(2034): 1563–1579.
- [6] Gourley, S.A. & Kuang, Y. 2004. A delay reaction-diffusion model of the spread of bacteriophage infection. *SIAM Journal on Applied Mathematics.* 65(2): 550–566.
- [7] Gourley, S.A., So, J.W.H. & Wu, J.H. 2004. Non-locality of reaction-diffusion equations induced by delay: biological modeling and nonlinear dynamics. *Journal of Mathematical Sciences.* 124(4): 5119–5153.
- [8] Gurney, W.S.C., Nisbet, R.M. & Lawton, J.H. 1983. The systematic formulation of tractable single-species population models incorporating age structure. *The Journal of Animal Ecology.* 52(2): 479–495.
- [9] Haag, K.H. 1986. Effects of herbicide application on mortality and dispersive behavior of the water hyacinth weevils, *Neochetina eichhorniae* and *Neochetina bruchi* (Coleoptera: Curculionidae). *Environmental entomology.* 15(6): 1192–1198.
- [10] Hill, M.P. & Olckers, T. 2001. Biological control initiatives against water hyacinth in South Africa: constraining factors, success and new courses of action. *Proceedings of the Second Meeting of the Global Working Group for the Biological and Integrated Control of Water Hyacinth.* Beijing, China, ACIAR proceedings No. 102. 33–38.
- [11] Howard, P. 2005. *Partial differential equations in MATLAB 7.0.* University of Maryland, College Park (MD).
- [12] Jones, R.W. 2009. *The impact on biodiversity, and integrated control, of water hyacinth, Eichhornia crassipes (Martius) Solms-Laubach (Pontederiaceae) on the Lake Nsezi - Nseleni River System.* PhD Dissertation. Rhodes University, Grahamstown.
- [13] Julien, M.H., Griffiths, M.W. & Wright, A.D. 1999. *Biological control of water hyacinth. The weevils Neochetina bruchi and N. eichhorniae: biologies, host ranges, and rearing, releasing and monitoring techniques for biological control of Eichhornia crassipes.* Australian Centre for International Agricultural Research (ACIAR) Monograph No. 60, Canberra.
- [14] Nuse, S. 2015. Consultant at Environmental Resource Management Department, Invasive Species Management, Westlake, [Personal Communication]. Contactable at sisanda.nuse@capetown.gov.za.
- [15] Penfound, W.T. & Earle, T.T. 1948. The biology of the water hyacinth. *Ecological Monographs.* 18(4): 447–472.
- [16] Powell, J. 2001. *Spatio-temporal models in ecology: an introduction to integro-difference equations.* Utah State University, Logan (UT).
- [17] Sargent, R.G. 2013. Verification and validation of simulation models. *Journal of Simulation.* 7: 12–24.
- [18] Süli, E. 2012. *Lecture notes on finite element methods for partial differential equations.* Mathematical Institute, University of Oxford, Oxford.
- [19] Taylor, C.M. & Hastings, A. 2005. Allee-effects in biological invasions. *Ecology Letters.* 8(8): 895–908.
- [20] The MathWorks Inc, . *MATLAB version 9.0 (R2016a).* [Computer Software], Natick (MA).
- [21] Wilson, J.R. 2002. *Modelling the dynamics and control of water hyacinth, Eichhornia crassipes (Martius) Solms-Laubach.* Unpublished PhD Dissertation. University of London. London.